A SIMULATION OF CO_2 UPTAKE IN A THREE DIMENSIONAL OCEAN CARBON CYCLE MODEL *

JIN Xin (金 心) and *SHI Guangyu* (石广玉)

LASG, Institute of Atmospheric Physics, Chinese Academy of Sciences, Beijing 100029

Received June 11, 2000

ABSTRACT

A three-dimensional ocean carbon cycle model which is a general circulation model coupled with simple biogeochemical processes is used to simulate CO_2 uptake by the ocean. The OGCM used is a modified version of the Geophysical Fluid Dynamics Laboratory modular ocean model (MOM2). The ocean chemistry and a simple ocean biota model are included. Principal variables are total CO_2, alkalinity and phosphate. The vertical profile of POC flux observed by sediment traps is adopted, the rain ratio, a ratio of production rate of calcite against that of POC, and the bio-production efficiency should be 0.06 and 2 per year, separately. The uptake of anthropogenic CO_2 by the ocean is studied. Calculated oceanic uptake of anthropogenic CO_2 during the 1980s is 2.05×10^{15} g (Pg) per year. The regional distributions of global oceanic CO_2 are discussed.

Key words: anthropogenic CO_2, ocean uptake, three-dimensional model, ocean carbon cycle model, regional distribution

I. INTRODUCTION

The partitioning of anthropogenic carbon amongst the reservoirs is an important problem in the study of global carbon cycle. There is no doubt that CO_2 concentrations in the atmosphere have increased from about 280 ppmv in pre-industrial times to 358 ppmv in 1994, according to the measurements in Mauna Loa, Hawaii, since 1958 and the ice core records over the past 1000 years. We also know, relatively firm, that this increase is largely due to fossil fuel combustion and cement production. By contrast, estimates of the oceanic sink and terrestrial biospheric source have large uncertainties associated with them, as the Intergovernmental Panel on Climate Change (IPCC) summary of these sources and sinks shows (Table 1). There are two aspects of the uncertainties. For one thing, the errors of the sources and sinks are very large. For example, the error of the oceanic sink is up to about 40%. For another, we have divided the Missing Sink into the uptake by Northern Hemisphere forest regrowth and the inferred sink (This inferred sink is consistent with independent estimates of carbon uptake due to nitrogen fertilization, plus the range of other uptakes due to CO_2 fertilization and climatic effects (Houghton et al. 1996)), but there are very large uncertainties in the constitution and the value of them.

* Supported by the National Natural Science Foundation of China (No. 49635200) and the National Key Program—Studies of Short-Range Climate Prediction System in China (No. 96-908-01-06).

In this paper the oceanic uptake of anthropogenic carbon is simulated by a three-dimensional ocean carbon cycle model. The regional distributions of global oceanic CO_2 are discussed and compared with the observations.

Table 1. The IPCC Anthropogenic Carbon Budget for 1980 to 1989 (Houghton et al. 1996)

CO_2 sources	Annual average (GtC/a)
Emissions from fossil fuel combustion and cement production	5.5±0.5
Net emissions from changes in tropical land-use	1.6±1.0
Total anthropogenic emissions partitioning amongst reservoirs	7.1±1.1
Storage in the atmosphere	3.3±0.2
Ocean uptake	2.0±0.8
Uptake by Northern Hemisphere forest regrowth	0.5±0.5
Inferred sink	1.3±1.5

II. MODEL DESCRIPTION

A three-dimensional ocean carbon cycle model, which is a general circulation model coupled with the ocean chemistry and simple biogeochemical processes, is used to simulate CO_2 uptake by the ocean (Jin and Shi 1999).

The ocean circulation model we used in this investigation is the configuration of a modified version of the Geophysical Fluid Dynamics Laboratory MOM2 (Pacanowski 1996). The topography of the model is obtained from the real global topography data, filtered five times locally. The equations are solved in a latitude, longitude, depth coordinate system using the Arakawa B grid. The model's space between grid points is 3° of latitude and 4° of longitude, and there are 15 vertical layers. The circulation was driven by the observed annual mean wind stress field, interpolated from the data set of Hellerman and Rosenstein (1983) and the observed surface values of salinity and temperature, taken from Levitus (1982). The restoring parameters of temperature and salinity have values of 1/(30 days) in the uppermost layer and zero everywhere below the surface layer. The model was spun up from a homogeneous initial state and run for 3000 years to an equilibrium state (Jin and Shi 2000).

In our model, the fact that the mixing process of CO_2 in the atmosphere is much faster than that in the ocean allows the atmosphere to be treated as one box. Prognostic variables of the model in the ocean are oceanic total CO_2 (TCO_2), total alkalinity (Talk), and phosphate (PO_4).

Sedimentation processes and river input due to the continental weathering are not included in our model. Therefore, the total amounts of phosphate and alkalinity are conserved in the ocean.

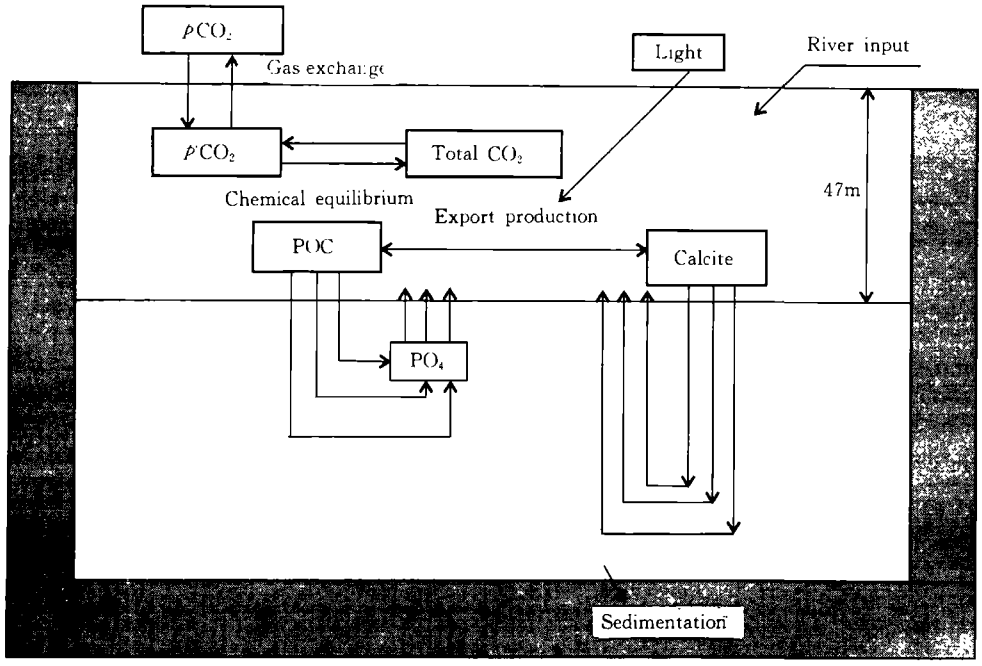

Fig. 1. Chemical and biological processes considered in the model. Processes of sedimentation and river input are not included (from Yamanaka 1996, the cycle of O_2 is not included).

The chemical and biological processes considered in the model are illustrated in Fig. 1. The partial pressure of CO_2 in the surface ocean is derived from total CO_2, alkalinity, temperature, and salinity. The apparent dissociation constants for carbon, borate, and water are taken from Dickson and Millero (1987), Johansson and Wedborg (1979), and Dickson and Riley (1979). The solubility of CO_2 is taken from Weiss (1974). The air-sea CO_2 flux is given by

$$S = k_g[(pCO_2)_o - (pCO_2)_a]. \quad (1)$$

For the experiment described in this paper, a constant value (Maier-Reimer 1993) $k_g = 0.06$ mol m^{-2} a^{-1} μatm^{-1} was chosen, matching Broecker's estimate.

The distribution of chemical tracers is affected by the biological activity. The most primary production is recycled in the surface water near where it was formed. A portion of primary production, called new production is transported to deeper water where it is remineralized. It is the new production that must be modeled. The new production EP is the function of the phosphate concentration $[PO_4]$ and light factor L_f (according to Michaelis-Menten kinetics, see Maier-Reimer 1993):

$$EP = rD_eL_f[PO_4]\frac{PO_4}{h + [PO_4]}, \quad (2)$$

where h is a half-saturation constant (Maier-Reimer 1993), taking 0.02 μmol L^{-1}; D_e is a depth of the surface layer, taking 47 m; r is a proportional factor, 2 a^{-1}. The light factor L_f depends on a latitudinally varying incident light, which is a simple function of latitude and is normalized to be $0 \leqslant L_f \leqslant 1$. In all processes where POC is involved, a constant Redfield ratio is assumed:

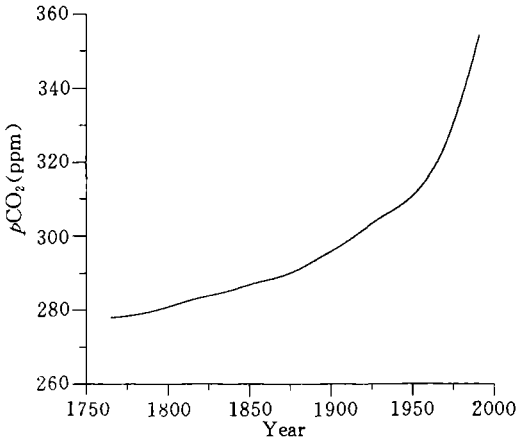

Fig. 2a. Spline fit to the Siple ice core/Mauna Loa atmospheric pCO_2 (Sarmiento et al. 1992).

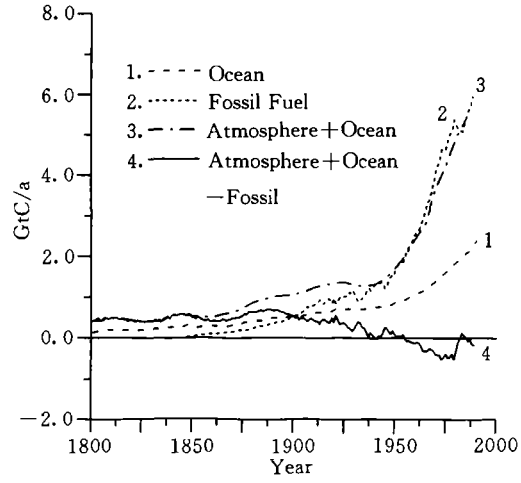

Fig. 2b. The annual change in carbon calculated by our model.

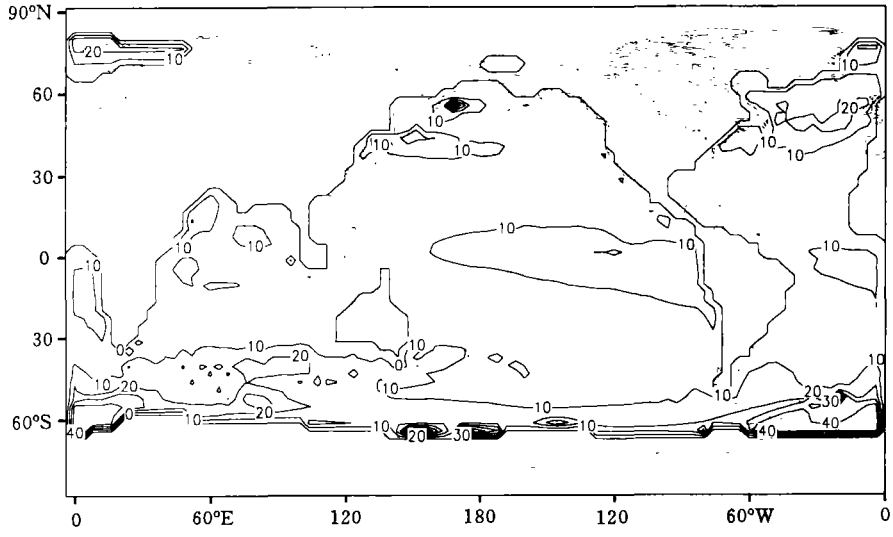

Fig. 3. A map of the atmosphere-ocean difference, $\Delta\delta pCO_2$, calculated by our model.

$$P : N : C : -O_2 = RP : RN : RC : RO = 1 : 16 : 106 : 138. \quad (3)$$

The value of the rain ratio R, a ratio of production rate of cacite to that of POC , is assumed to be 0.06.

The vertical profile of POC flux is represented in the form of

$$F = \left(\frac{z}{100}\right)^a, \quad (4)$$

where $a = 0.858$ (this profile is taken from vertical flux of particulate organic nitrate obtained from the sediment traps, see Martin et al. (1987). POC is assumed to be remineralized instantaneously below the euphotic zone and equals $-dF(z)$. Calcite is assumed to dissolve uniformly below the depth of 1500 m. Since the sedimentation process

is not included in our model, the amounts of POC and calcite which are precipitated into the bottom box are added into the surface box to keep the conservation of phosphate and alkalinity.

III. GLOBAL OCEANIC CO_2 UPTAKE AND REGIONAL DISTRIBUTIONS

The Siple ice core/Mauna Loa atmospheric pCO_2 which is used to force the simulation is illustrated in Fig. 2a. and Fig. 2b shows the annual change in carbon calculated by our model. Siegenthaler and Oeschger (1987), Keeling et al. (1989a) and Sarmiento and Orr (1992) have discussed similar figures that they obtained from their studies. In the early nineteenth century, because there were major CO_2 emissions from deforestation starting before 1800 (Siegenthaler and Oeschger 1987), a relatively large annual input to the atmosphere is necessary in order to explain the atmospheric CO_2 concentration increase at that time.

After 1951 the combined oceanic and atmospheric uptake of carbon by our model is less than the fossil production as estimated by Keeling (1991) and Marland and Boden (1991). From 1958 to 1990, the combined atmospheric and oceanic increase of 135.5 GtC ($1Gt=10^{12}$ kg$=1$ Pg) is 5.5% lower than the estimated fossil CO_2 production of 143.48 GtC. In order to account for the fossil source during these years the oceans have to take up 15% more CO_2. During this period the emission of CO_2 by land use is 45.70 GtC (calculated by the data of Houghtond, see Enting et al. 1994). Therefore, the combined atmospheric and oceanic increase accounts for 72% emission, about 2/3 of the total. the sources include the fossil production, deforestation and the land use.

Before we discuss the regional distributions of oceanic CO_2 uptake, we first give the following definitions:

$$\Delta\delta pCO_2 = \Delta pCO_2 - \Delta pCO_{2,0} = \delta pCO_{2OC} - \delta pCO_{2atm}, \tag{5}$$

$$\Delta pCO_2 = pCO_{2OC} - pCO_{atm}, \tag{6}$$

$$\delta pCO_2 = pCO_2 - pCO_{2,0} \tag{7}$$

where δpCO_2 is the cumulative change at time t relative to pre-anthropogenic, ΔpCO_2 is the air-sea difference, and $\Delta\delta pCO_2$ is that portion of the air-sea difference at time t.

The air-sea flux of CO_2 is mainly determined by the air-sea difference, $\Delta\delta pCO_2$, at time t. Figure 3 shows the map of the air-sea difference, $\Delta\delta pCO_2$. The pattern of $\Delta\delta pCO_2$ derives primarily from the different type of convective overturning and upwelling. There are strong equatorial and subpolar upwelling as well as high-latitude convection. Compared with the maps of vertical velocity, we can conclude that the high values of air-sea difference $\Delta\delta pCO_2$ correspond with the intensity of vertical motion in these regions, e.g., there are high values in the equatorial and subpolar upwelling regions.

Figure 4 shows the zonal mean annual anthropogenic CO_2 air-sea flux in 1990 in our mode. The ocean uptake of anthropogenic CO_2 is different in different latitudes. This result is similar to that of the other 3-D ocean general circulation model studies of oceanic uptake in which the biological process is not included (Sarmiento and Sundquist 1992). There are maximum values in the equatorial and subtropics regions. This is because that the water that upwells at the equator has been out of contact with the atmosphere for a considerable amount of time and thus has only a small excess anthropogenic CO_2 load

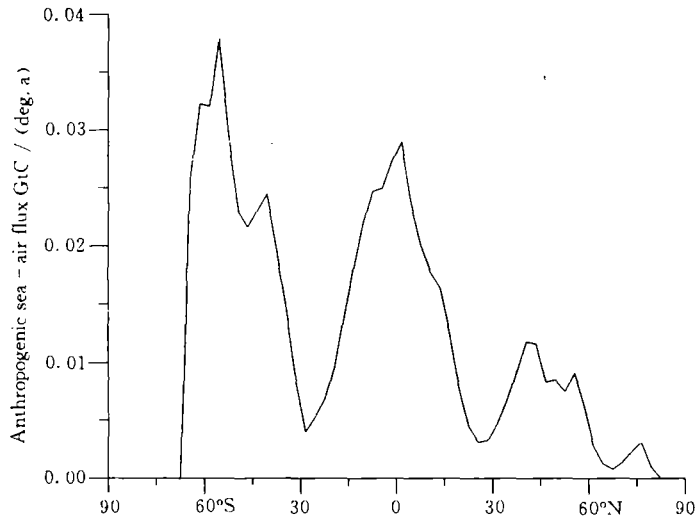

Fig. 4. The zonal mean annual air-sea flux in 1990 in our model.

picked up when it was last in contact with the atmosphere (Sarmiento and Sundquist 1992). The maximum value in the southern ocean region caused mainly by the fact that there are very large ocean areas in these latitudes.

Of course, the anthropogenic CO_2 which entered into the ocean does not simply stay in the region where it is added to the ocean. but is redistributed horizontally. Figure 5 shows the maps of the cumulative input and standing crop in our model. Figure 6 shows the zonal integral flux and standing crop in our model. We can see from the figures that the anthropogenic CO_2 in the ocean is lost from the equatorial regions and subpolar gyres and accumulate primarily in the subtropical gyres. This meridional redistribution is controlled predominantly by upwelling of waters in the equatorial region and subpolar gyre.

A useful diagnostic of how much the oceanic uptake contributes to the total carbon budgets is the airborne fraction for the combined atmosphere and ocean:

$$AF_{ao} = \frac{(I_t^{atm} - I_0^{atm})}{(I_t^{atm} - I_0^{atm}) + (I_t^{OC} - I_0^{OC})}, \tag{8}$$

where I^{atm} and I^{oc} are the atmospheric and oceanic inventory in Pg of carbon, separately. $t=0$ is the beginning of the simulation. Table 2 gives a comparison of our model with the box diffusion model (Siegenthaler and Oeschger 1987) and 3-D model (Sarmiento and Sundquist 1992). The airborne fractions given by the box-diffusion and outcrop-diffusion models are 0.581 and 0.479, respectively, for the period 1959—1983. Both are lower than the value of our model (0.608), and the value of 3-D (0.617) is a little larger than ours. The modeling result for the period 1980 — 1989. annual mean oceanic uptake of anthropogenic CO_2 is 2.05 GtC , which corresponds with the value in Table 1.

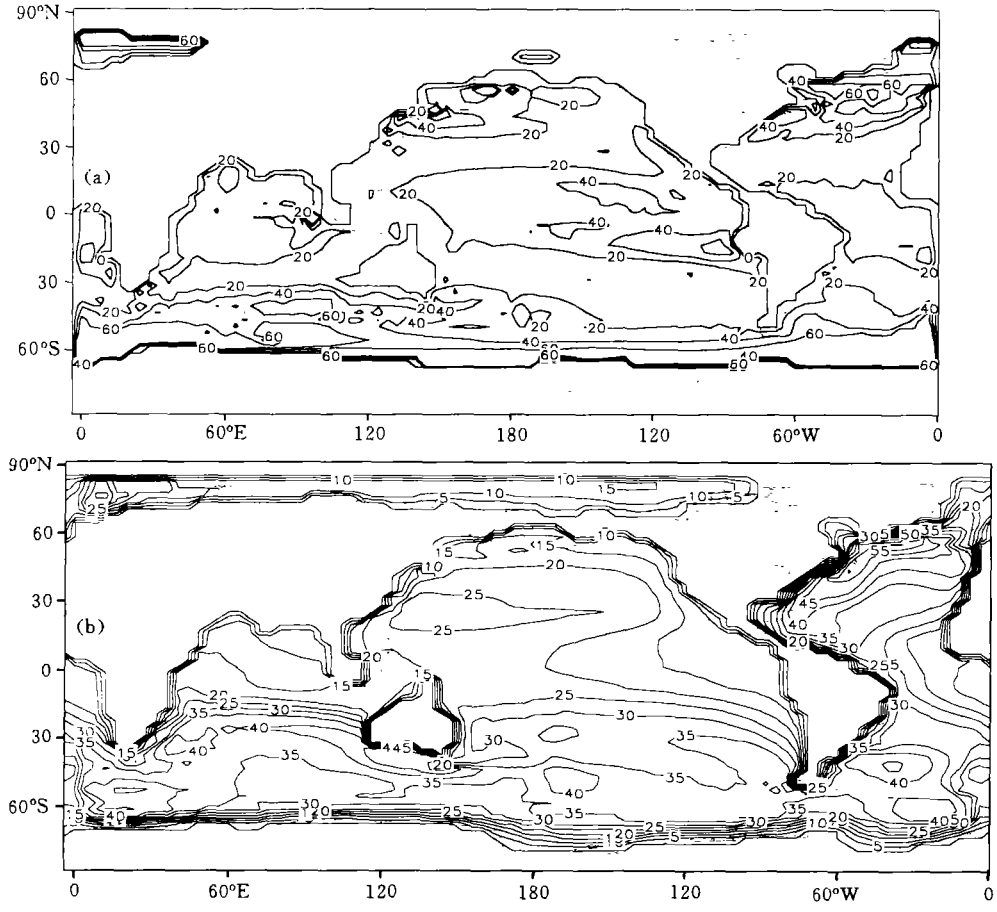

Fig. 5. A map of the cumulative input (mol m^{-2}) of anthropogenic CO_2 (a) and a map of the standing crop (mol m^{-2}) calculated by our model (b).

Table 2. Airborne Fraction (Prescribed Atmospheric CO_2 Concentration) for Different Models

	Box diffusion	Outcrop diffusion	3-D	Our model
1970—1980	0.510	0.405	0.582	0.551
1959—1983	0.581	0.479	0.617	0.608

It is difficult to get an observation map of oceanic uptake of anthropogenic CO_2, for the quality and number of oceanographic carbon system measurements are severely limited. Here we compared the model results with the observation one in a few latitude regions. Tans et al. (1990) estimates oceanic uptake of CO_2 based on measurements of air-sea CO_2 difference for the period between 1972 and 1989. Table 3 gives the comparison of our model result and the estimates of Tans et al. The feature of the oceanic uptake of CO_2 given by our model is in agreement with the data-based estimates. There is a strong source in equatorial band. There is a strong sink in subtropics of the Southern and Northern Hemispheres. Our model gives an average uptake of 1.81 GtC/a for the period between

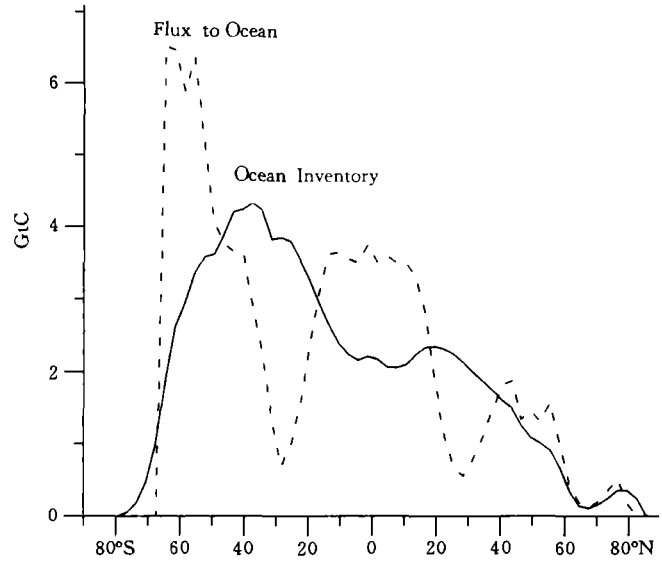

Fig. 6. Zonal integral (3 deg.) flux and standing crop from our model.

1972 and 1989, in good agreement with the data-based estimates, 1.88 GtC/a. However, a large Southern Hemisphere sink is inconsistent with results obtained from atmospheric models.

Table 3. Comparison of Tans et al. (1990) Air-Sea Fluxes with Our Model Results

Regions	Tans	Our model
>15°N	−0.59	−0.95
15°S−15°N	+1.30	+0.85
50−15°S	−2.39	−1.20
90−50°S	−0.20	−0.51
Total	−1.88	−1.81

The large Southern Hemisphere oceanic sink which is suggested by data-based estimates requires a large interhemispheric CO_2 transport within the atmosphere from fossil CO_2 sources in the Northern Hemisphere, even after the geographical distribution of terrestrial biota sources and sinks is taken into consideration. Such a transport is not supported by 3-D atmospheric transport models constrained with the observed interhemispheric CO_2 gradient (Tans et al. 1990).

Tans et al. (1990) solve this difficulty in their scenarios 5 to 8 by ignoring the data-based Southern Hemisphere air-sea exchange flux estimates, while accepting those in the Northern Hemisphere, arguing that the former is rather poorly constrained by the data (Sarmiento 1992). These scenarios give a total oceanic uptake of only −0.3 to −0.8 GtC/a for the periods 1981−1987. Hence Tans et al. conclude that the oceanic uptake is at most −1 GtC/a. This is in contrast to the results of Table 1.

Keeling et al. (1989b) 3-D atmospheric CO_2 transport model is not able to support a large interhemispheric transport of CO_2 either. However, they solve the problem by putting a large flux of CO_2 into the Northern Hemisphere ocean primarily by adjusting their pre-industrial air-sea flux estimates. Their final scenario has a total oceanic uptake flux for 1984 of -2.30 GtC/a. and net terrestrial sink of only -0.46 GtC/a. both of which are close to the values in Table 1. and in good agreement with our ocean model results. Keeling et al. are also in agreement with Scenarios 1 and 2 of Tans et al.

Table 4. Comparison of Tans et al. (1990) Air-Sea Fluxes with Keeling et al. (1989b)

Tans				Keeling (1989b)	
Region	Data	Scenarios 1 and 2	Scenarios 5 to 8	Region	Scenario
>15°N	−0.6	−2.4	−0.6	>15.6°N	−2.3
15°S−15°N	+1.6	+1.0	+1.3	15.6°S−15.6°N	+1.1
50−15°S	−2.4	−1.2	−1.7	39.1−15.6°S	−1.1
90−50°S	−0.2	+0.5	+0.5	90−39.1°S	+0.0
total	−1.6	−2.1	−0.5	total	−2.3

Analyzing the issues of Tans et al. about the carbon cycle, Toggweiler (1995) concluded that the ocean is naturally transporting carbon across latitude circles or between the hemispheres. Meridional transports within the ocean imply that there are natural CO_2 fluxes between the ocean and atmosphere which influence atmospheric CO_2 gradient. The ocean and land also exchange carbon (via rivers). These aspects of the natural cycle are not taken into account in the Tans et al. analysis. The conclusion of Keeling et al.. which the ocean is naturally transporting carbon across latitude circles from Northern Hemisphere to Southern Hemisphere, is basically correct.

We compare our model result of pre-industrial air-sea flux with the assumption of Keeling et al. (as in Table 5) which is to say that anthropogenic CO_2 is being added to a system in which the atmosphere naturally transports CO_2 from the Southern Hemisphere to the north and the release of fossil fuel CO_2 in the Northern Hemisphere currently overwhelms the natural interhemispheric cycle and reverses the atmospheric gradient. Our model results are in good agreement with the one of Keeling et al. between 15.6°N and 39.1°S.

we do not consider the river input of CO_2, about 0.8 GtC (Sarmiento et al. 1993).

If we add the river input into the Northern Hemisphere, increase the intensity of the North Atlantic Deep Water. Then the ocean will uptake more anthropogenic CO_2 in the Northern Hemisphere and then transports it to the Southern Hemisphere. Therefore our model results of pre-industrial demonstrate partly the assumption of Keeling (1989b).

Table 5. Comparison of Our Model' s Result in Pre-industrial Air-Sea Flux with Keeling et al.

Regions	Keeling (1989b)	Our model
>15.6°N	−1.69	−0.7
15.6°S−15.6°N	+1.83	+1.6
39.1−15.6°S	−0.58	−0.6
90−39.1°S	+0.44	−0.3
total	0.0	0.0

IV. CONCLUSION

A three-dimensional ocean carbon cycle model, which is a general circulation model coupled with simple biogeochemical processes, is used to simulate CO_2 uptake by the ocean. Model results show that the combined atmospheric and oceanic increase accounts for 72% emission, about 2/3 of the total. the sources include the fossil production. deforestation and the land use. Calculated oceanic uptake of anthropogenic CO_2 during the 1980s is 2.05 Pg per year; the oceanic anthropogenic CO_2 shows strong feature of regional distributions of global oceans. there are maximum values in the equatorial and subtropics regions; The feature of the oceanic uptake of CO_2 given by our model is in agreement with the data-based estimates; the distribution of oceanic uptake of CO_2 in pre-industrial period demonstrates the assumption of Keeling et al. —the carbon is transported from Northern Hemisphere to Southern Hemisphere in the ocean, but in the atmosphere the carbon is transported from Southern to Northern Hemisphere.

REFERENCES

Dickson, A. G. and Millero, F. J. (1987), A comparison of the equilibrium constants for the dissociation of carbonic acid in sea water media, *Deep Sea Res.*, **34**: 1733−1743.

Dickson, A. G. and Riley, J. P. (1979), The estimation of acid dissociation constants in seawater media from potentiometric titrations with strong base. I. The ionic product of water (Kw). *Mar. Chem.*, **7**: 89−99.

Enting, I. G., Wigley, T. M. L. and Heimann, M. (1994), Future emissions and concentrations of carbon dioxide: Key Ocean/ Atmosphere / Land Analyses, CSIRO Aust. Div. Atmos. Res. Tech. Pap. No. 31.

Hellerman, S. and Rosenstein, M. (1983), Normal monthly wind stress over the world ocean with error estimates, *J. Phys. Oceanogr.*, **13**: 1093−1104.

Houghton, J. T., Meira Filho, L. G., Callander, B. A., Harris, N., Kattenberg, A. and Maskell, K. (1996), *Climate Change* 1995. The IPCC Scientific Assessment, Cambridge University Press, New York, 1996.

Jin Xin and Shi Guangyu (1999), Numerical modeling for distribution of carbon and nutrient in the ocean. *Climatic and Environmental Research*, **4**: 375−387.

Jin Xin and Shi Guangyu (2000), A simulation of nature and bomb radiocarbon in global ocean general circulation models, *Chinese J. Atmos. Sci.*, **24**: 341−354.

Johansson, Q. and Wedborg, M. (1979), On the evaluation of potentiomatric titrations of seawater with

hydrochloric acid. *Acta Oceanologica Sinica*, **5**: 209—218.

Keeling, C. D., Bacastow, R. B., Carter, A. F., Piper, S. C., Whorf, T. P., Heimann, M., Mook, W. G. and Roeloffzen, H. (1989a). A three dimensional model of atmospheric CO_2 transport based on observed winds. 1. Analysis of observational data. in Aspects of Climate Variability in the Pacific and the Western Americas, edited by D. H. Peterson. pp. 165—236. *Geophys. Monogr.*, 55., AGU, Washington, D. C.

Keeling, C. D., Piper, S. C. and Heimann, M. (1989b). A three dimensional model of atmospheric CO_2 transport based on observed winds. 4. mean annual gradients and interannual variations. in Aspects of Climate Variability in the Pacific and the Western Americas, *Geophys. Monogr.*, 55, edited by D. H. Peterson. pp. 305—363, AGU, Washington, D. C.

Keeling, C. D. (1991), CO_2 emissions—Historical Record, pp. 383—385 of Trends' 91: *A Compendium of Global Change*. Eds. T. A. Boden, R. J. Sepanski and F. W. Stoss. (Carbon Dioxide Information and Analysis Center: Oak Ridge).

Levitus, S. (1982). *Climatological Atlas of the World Ocean*, NOAA Prof. Pap. 13. U. S. Government Printing Office, Washington, D. C.

Maier-Reimer, E. (1993): Geochemical cycles in an ocean general circulation model. Preindustrial tracer distributions., *Global Biogeochem. Cycles*, **7**: 645—677.

Marland, G. and Boden, T. (1991), CO_2 emissions—Historical Record. pp 383—385 of Trends '91: *A Compendium of Global Change*. Eds. T. A. Boden, R. J. Sepanski and F. W. Stoss. (Carbon Dioxide Information and Analysis Center: Oak Ridge).

Martin, J. H., Knauer, G. A., Karl, D. M. and Broenkow, W. W. (1987), VERTEX: Carbon cycling in the northeast Pacific, *Deep Sea Res.*, **34**, 267—285.

Sarmiento, J. L. and Orr, J. C. (1992). A perturbation simulation of CO_2 uptake in an Ocean General Circulation model. *J. Geophys. Res.*, **97**: 3621—3645.

Sarmiento, J. L. and Sundquist, E. (1992). Revised budget for the oceanic uptake of anthropogenic carbon dioxide. *Nature*, **356**: 589—593.

Siegenthaler, U. and Oeschger, H. (1987). Biosphere CO_2 emissions during the past 200 years reconstructed by deconvolution of ice core data. *Tellus*, **39**B: 140—154. 1987.

Tans, P. P., Fung, Y. and Takahashi, T. (1990). Observational constraints on the global atmospheric CO_2 budget. *Science*, **247**: 1431—1438.

Toggweiler, J. R. (1995), Anthropogenic CO_2: The natural carbon cycle reclaims. *Reviews of Geophysics*, Supplement. 1249—1252.

Weiss, R. F. (1974). Carbon dioxide in water and seawater: the solubility of non-ideal gas, *Mar. Chem.*, **2**: 203—215.

Yamanaka, Y. (1996), Development of ocean biogeochemical general circulation model. Center for Climate System Research University of Tokyo. Report No. 1.